Propellants by Regenerative and External Means," *Jet Propulsion*, Vol. 25, No. 12, 1955, pp. 707–711.

[5]Seifert, H., and Altman, D., "A Comparison of Adiabatic and Isothermal Expansion Processes in Rocket Nozzles," *ARS Journal*, Vol. 22, No. 3, 1952, pp. 159–162.

[6]Kanmuri, A., Kanda, T., Wakamatsu, Y., Torii, Y., Kagawa, E., and Hasegawa, K., "Transient Analysis of LOX/LH2 Rocket Engine (LE-7)," AIAA Paper 89-2736, July 1989.

[7]Mayer, E., "Analysis of Convective Heat Transfer in Rocket Nozzles," *ARS Journal*, Vol. 31, No. 7, 1961, pp. 911–917.

[8]Schlichting, H., "Boundary Layer Theory," McGraw-Hill, New York, 1979, p. 610.

[9]Shapiro, A. H., "The Dynamics and Thermodynamics of Compressible Fluid Flow: Vol. I," Ronald, New York, 1953, pp. 229–232.

Performance Evaluation of LE-7 High-Pressure Pumps

Kenjiro Kamijo* and Makoto Yoshida†
National Aerospace Laboratory, Kakuda, Miyagi 981-15, Japan
and
Takaharu Nagao‡
National Space Development Agency of Japan, Minatoka, Tokyo 105, Japan

I. Introduction

A LARGE launch vehicle, the H-II, has been developed in Japan. The launch vehicle uses a LOX/LH_2 engine, the LE-7, the thrust of which is about 1000 kN. The cryogenic propellant feed pumps of the LE-7 engine are characterized by high delivery pressure and large flow rate. The hydrodynamic performance of these pumps was thermodynamically evaluated mainly for the following reasons:

1) With regard to compressible fluids, the pump performance evaluations, which are based on assumptions of incompressibility, do not necessarily show the true pump performance because a fair amount of energy input to a pump is spent on increasing the internal energy.

2) With regard to pump efficiency measurement, a torquemeter could not be installed between the pump and the turbine of a turbopump. The installation of a torquemeter complicates turbopump assemblies to such a degree that they are not able to operate at the rated rotational speed.

The efficiency of the LOX pump was evaluated based on the adiabatic efficiency[1,2] because LOX is not so compressible. However, the efficiency directly determined from the measured pressures and temperatures was corrected for internal leakage from the split pump to the main pump.

With regard to the LH_2 pump performance, the polytropic head and efficiency which has been used as the true aerodynamic efficiency[3] were examined, because LH_2 is much more compressible than LOX. Since it was impossible to know the detailed compression process in a pump, a simplified calculation was carried out to determine the polytropic head and efficiency.

Received Sept. 23, 1991; revision received Oct. 22, 1992; accepted for publication June 3, 1993.

*Head, Rocket Fluid Systems Section, Kakuda Research Center. Member AIAA.

†Researcher, Rocket Fluid Systems Section, Kakuda Research Center. Member AIAA.

‡Assistant Senior Engineer, Propulsion Engineering Group, 2-4-1, Hamamatsu-cho.

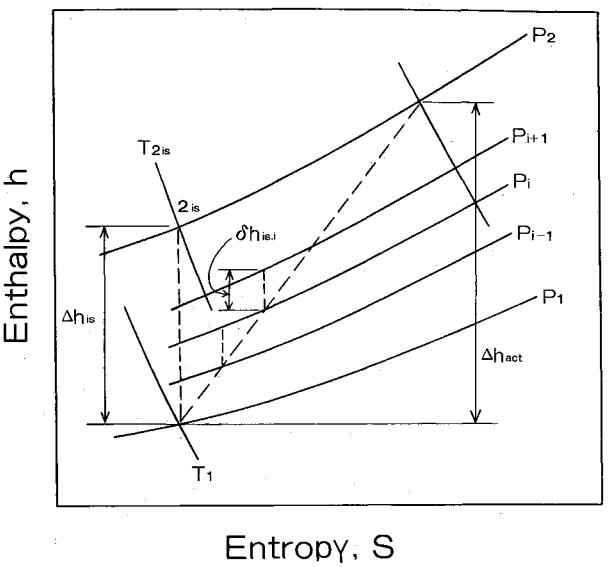

Fig. 1 Compression process of pump fluid.

II. Polytropic Head and Efficiency

A typical compression process of cryogenic fluids is presented in Fig. 1 using an enthalpy h—entropy s diagram. p_1 and p_2 represent the pump inlet and outlet pressure, respectively. The isentropic and actual compression processes are indicated by dotted lines. The adiabatic efficiency is presented by the following equation in which both the kinetic and geodetic heads are neglected:

$$\eta_a = (\Delta h_{is}/\Delta h_{act}) \tag{1}$$

where Δh_{is} and Δh_{act} are the increase of enthalpy in the isentropic compression process and the energy input to the pump, respectively. Since it was impossible to know the detailed compression process in a pump, the polytropic head and efficiency are calculated by the following expedient procedures. An isentropic compression process with a fixed efficiency is assumed between all the adjacent isobaric lines which are drawn between the two isobaric lines of pressures p_1 and p_2 as shown in Fig. 1. The polytropic head Δh_{tr} is obtained as the sum total of all isentropic enthalpy increments between the adjacent isobaric lines:

$$\Delta h_{tr} = \Sigma \delta_{is,i} \tag{2}$$

The polytropic efficiency is defined as follows:

$$\eta_{tr} = (\Delta h_{tr}/\Delta h_{act}) \tag{3}$$

As shown in Fig. 1, the enthalpy increment between the adjacent isobaric lines increases with the increase of entropy. So both the polytropic head and efficiency result in larger values than those of the adiabatic head and efficiency.

III. Test Pumps and Test Procedures

The major design parameters of the LOX and LH_2 pumps of the LE-7 engine are presented in Table 1. The impellers of the main pump and the split pump are arranged on a common shaft with the LOX pump. The main pump has an inducer with three swept-back blades. The split pump sucks in about 20% of the delivery of the main pump. There is internal leakage from the split pump to the main pump through the wearing ring seal. The LH_2 pump is a two-stage centrifugal pump with an inducer which is similar to that of the LOX pump. Each of the main impellers has 10 full vanes and 10 partial vanes.

Table 1 Design parameters of LE-7 propellant feed pumps

	LOX Pump		LH_2
	Main	Split	Pump
Rotational speed, rpm	20,000	20,000	46,130
Shaft power, kW	5,222	662	22,065
Stage specific speed, m, m^3/s, s^{-1}	0.0947	0.0644	0.0562
Mass flow, kg/s	229.0	43.8	38.9
Volume flow, l/s	201.0	38.4	563.0
Inlet pressure, MPa	0.40	20.1	0.32
Outlet pressure, MPa	21.3	32.7	31.5

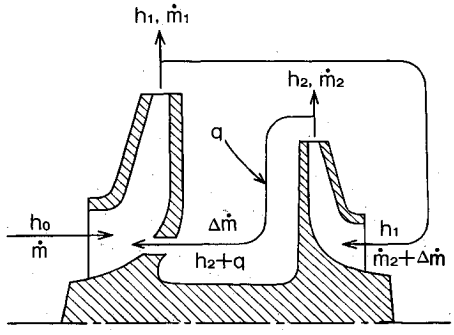

Fig. 2 Internal flow of main and split pump.

The pressures and temperatures at the pump inlet and outlet were measured to obtain the enthalpies which are necessary to thermodynamically calculate the pump performance. All the pressures were measured by strain-gauge-type sensors. Temperature measurements of LOX and LN_2 were carried out with C-C thermocouples which were calibrated using LN_2. LH_2 temperatures were measured with platinum resistance thermometers. Fluid properties, which were necessary to obtain the pump performance, were according to Ref. 4. All the flow rates were measured by turbine-type flow meters.

IV. Performance of the LOX and LH_2 Pumps

Since there is internal leakage from the split pump to the main pump as shown in Fig. 2, the influence of this leakage on the performance of both pumps must be considered with the LOX pumps. The measured adiabatic efficiencies of the main and the split pump were obtained utilizing the measured temperatures and pressures of both the pump inlet and outlet. These efficiencies are represented by the following equations:

$$\eta^*_{a,m} = \frac{h_{1is} - h_0}{h_1 - h_0} \tag{4}$$

$$\eta^*_{a,s} = \frac{h_{2is} - h_1}{h_2 - h_1} \tag{5}$$

The mass flow of the internal leakage from the split pump to the main pump through the wearing ring seal is designated as $\Delta\dot{m}$, which is determined by calculation utilizing the measured pressure distribution within both the pumps. q is the enthalpy increment of the leakage flow which is caused by the disc friction loss of the back shroud of the split pump impeller. The measured efficiencies ($\eta^*_{a,m}$, $\eta^*_{a,s}$) are corrected for the internal leakage flow by the following equations using the symbols in Fig. 2:

$$\eta_{a,m} = \frac{\eta^*_{a,m}}{1 - \dfrac{\Delta\dot{m}}{\dot{m}_1}\dfrac{h_2 - h_1 + q}{h_1 - h_0}} \tag{6}$$

$$\eta_{a,s} = \frac{\eta^*_{a,s}}{1 + \dfrac{\Delta\dot{m}}{\dot{m}_2}\dfrac{h_2 - h_1 + q}{h_2 - h_1}} \tag{7}$$

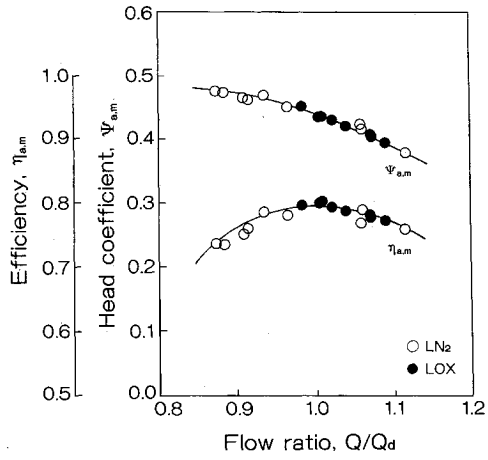

Fig. 3 Performance of LOX main pump at rated rotational speeds.

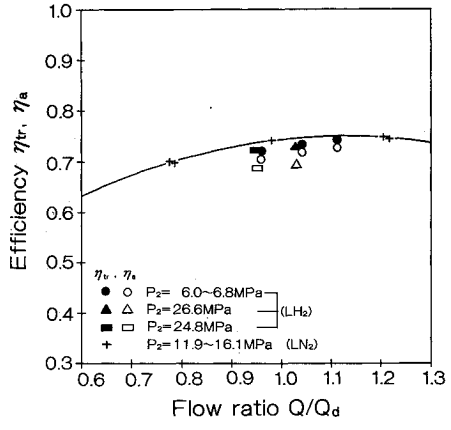

Fig. 4 LH_2 pump efficiency and comparison of adiabatic and polytropic efficiencies.

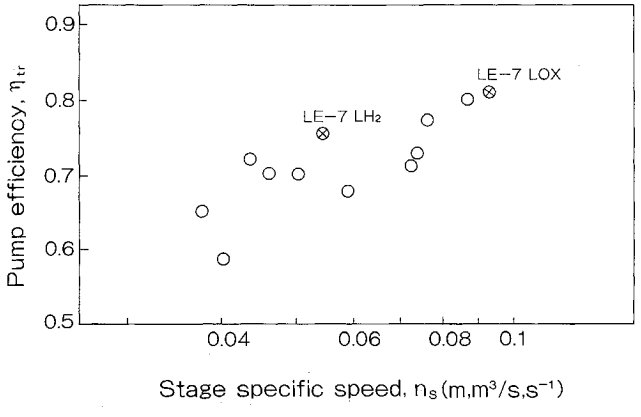

Fig. 5 Efficiency of large rocket pumps.

It was confirmed that the measured adiabatic heads and the measured ordinary heads of the LOX pump fairly well agreed in the tests in which the pump pressure rises were less than 10 MPa, indicating that the influence of compressibility on the pump efficiencies or heads ought to be less than 0.5%. This verified that the temperatures and pressures were measured with high accuracy in the present test. Figure 3 presents the performance of the main pump obtained at the rated rotational speeds. The scattering of the efficiency in this figure falls within a range of a few percent, which verified the usefulness of thermodynamic evaluation of pump performance, even with LOX and LN_2, which show comparatively small compressibility.

Test results of the LE-7 LH_2 pump are presented in Fig. 4. With regard to LN_2, the performance was represented by

the adiabatic efficiency which is considered to closely approximate the true performance because the delivery pressure in the LN_2 tests was less than 16 MPa. With regard to LH_2, not only the adiabatic efficiency, but also the polytropic efficiency, is presented in Fig. 4. The polytropic efficiency fairly well agreed with the head and efficiency obtained in the LN_2 test. Based on the above mentioned fact, the polytropic efficiency can be considered to show nearly true pump head and efficiency.

The efficiency of about 80% at the designed flow ratio ($Q/Q_d = 1.0$) with the LOX pump mentioned above is considered to be fairly high compared with those of the previously developed rocket pumps as shown in Fig. 5.[5] Figure 5 shows the stage efficiency of the rocket pumps with the main impeller, the diameter of which was more than 195 mm. The efficiency of about 75% obtained with the present LH_2 pump can also be considered as reasonable as shown in Fig. 5.

Acknowledgment

The authors are grateful for the help of Yasuko Sato of the Rocket Fluid Systems Section of the National Aerospace Laboratory, Miyagi, Japan.

References

[1]Diem, H. G., "Recent Progress on the Advanced Space Engine," AIAA Paper 78-940, July 1978.

[2]Kamijo, K., and Hirata, K., "Performance of Small High Speed Cryogenic Pumps," *Transactions of the American Society of Mechanical Engineers, Journal of Fluids Engineering*, Vol. 107, No. 2, 1985, pp. 197–204.

[3]Balje, O. E., *Turbomachine*, John & Sons, Inc., 1983, pp. 10–15.

[4]McCarty, R. D., "Interactive Fortran IV Computer Programs for the Thermodynamic and Transport Properties of Selected Cryogens [Fluid Pack]," National Bureau of Standards TN 1025, 1980.

[5]Anon., "Liquid Rocket Engine Centrifugal Flow Turbopumps," NASA SP-8109, Dec. 1973, pp. 15–17.

Numerical Prediction of a Turbulent Evaporating Fuel Spray in a Recirculating Flow

Xi-Qing Chen* and José Carlos Fernandes Pereira†
Instituto Superior Técnico/Technical University of Lisbon, 1096 Lisbon Codex, Portugal

Introduction

INVESTIGATION of turbulent evaporating sprays is vitally important in various industrial applications, such as industrial combustors, gas turbines, etc. With the advent of high-speed and sophisticated computers, numerical modeling has been playing a more and more important role. Up to now, various mathematical and physical models have been developed to predict the flow characteristics of sprays. Due to the intrinsic existence of potential multivaluedness arising as droplet trajectories cross, the Lagrangian separated-flow methods are widely used. Currently used spray combustion models have been reviewed.[1–5]

Received Oct. 13, 1992; revision received March 8, 1993; accepted for publication April 17, 1993.

*Ph.D. Student, Mechanical Engineering Department, Av. Rovisco Pais.

†Associate Professor, Mechanical Engineering Department, Av. Rovisco Pais. Member AIAA.

The Lagrangian approach[6] treats the dispersed phase by representing different droplet "parcels," each of which is assumed to possess the same size range, diameter, and velocity. The droplet motion is governed by the Lagrangian form of transport equations. In tracking each parcel of droplets, the loss or gain of droplet mass, heat, and momentum within each Eulerian cell can be obtained, which will be used as the coupling source or sink terms in the corresponding finite difference equations for the gas phase. Lagrangian treatment of droplet transport possesses the advantages of no numerical diffusion and easy treatment of multivaluedness. But if this approach is used to track the droplet motion in a deterministic way, the advantage of no numerical diffusion will turn out to be its disadvantage as well, which gives a discernible underprediction of droplet dispersion. Confronted with this problem, many researchers are presently employing the stochastic separated-flow (SSF) method to treat the gas-turbulence influence on the droplet motion through particle-eddy interactions.[7] This method has wide applications and gives encouraging results in a variety of flow situations,[8–10] including flows with and without evaporation.

While the SSF models have found wide acceptance and been applied with great success in most spray combustion modeling, they usually neglect the fact that turbulent velocity fluctuations are correlated temporally and directionally, and vanish only when the time elapsed is large and cross-correlations are zero. To account for this physical phenomenon in practical spray combustion modeling, Berlemont et al.[11] and Zhou and Leschziner[12] have recently proposed two similar models to incorporate the turbulent temporal correlations and anisotropy, both of which share the same philosophy, but start from different routes.

In this Note, a comprehensive spray evaporation model, based on an Eulerian model of the gas field and a Lagrangian model of the droplet field in conjunction with the stochastic description of gas turbulence effect on the droplet motion, is applied to a turbulent evaporating spray in a recirculating flow and validated by comparison between predictions and measurements. Unlike many previous numerical predictions, this Note has been able to avoid the usual problem of a lack of detailed initial droplet-size and velocity-distribution conditions, and incorporated the turbulent temporal and directional correlations. In the present study, we have adopted Zhou and Leschziner's methodology to include turbulent temporal and directional correlations in the numerical modeling, which has proved to be an improvement over the conventional particle-eddy modeling in simple flows.[13,14]

Physical Model Description

We consider an evaporating spray of liquid isopropyl alcohol issuing into a coflowing turbulent, heated, airstream. An annular air jet enters the test section of 194-mm i.d. The inlet air and liquid isopropyl alcohol temperatures are 353 and 304 K, respectively. The detailed droplet-size and velocity distribution data were measured with phase-Doppler by Sommerfeld.[15]

Governing Equations for the Gas Field and Droplet Field

The equations for the continuous gas field are based on the modified two-equation turbulent eddy-viscosity model by incorporating two-phase coupling source terms. Application of the Reynolds time-averaging process to the Eulerian form of conservation equations for each dependent variable results in the mean flow equations for all dependent variables.

The droplet field is calculated by tracking the droplet parcels throughout the computational domain. The initial droplet-size distribution of the spray is divided, according to the given experimental probability density function (PDF), into an adequate number of discrete parcels, each of which represents a set of droplets belonging to the same size range and possessing the same initial conditions. Due to the small ratio